

Country-level energy demand for cooling has increased over the past two decades

Enrico Scoccimarro ¹✉, Oreste Cattaneo¹, Silvio Gualdi¹, Francesco Mattion², Alexandre Bizeul², Arnau Martin Risquez² & Roberta Quadrelli²

Cooling degree days provide a simple indicator to represent how temperature drives energy demand for cooling. We investigate, at country level, the changes in cooling degree days worldwide in a recent twenty-one-year period starting in 2000. A new database, jointly generated by CMCC and IEA based on ERA5 reanalysis' global gridded data, is used for the analysis. In contrast to the existent literature, the factors of population-weighting and humidity are considered, which affect the magnitude and the spatial distribution of these changes. Annual tendencies show a general increase of cooling degree days over the different countries, fostering more energy consumption for cooling demand, as confirmed by some regional studies. We also focus on the temporal clustering, to measure if peaks occur evenly random or tend to cluster in shorter periods. We stress that including humidity is important both for general tendencies and clustering. India, Cambodia, Thailand and Vietnam represent the emerging countries where this effect is stronger.

¹Fondazione Centro Euro-Mediterraneo sui Cambiamenti Climatici (CMCC), Bologna, Italy. ²International Energy Agency (IEA), Paris, France.
✉email: enrico.scoccimarro@cmcc.it

Population growth and global warming are imposing a major challenge for the future energy supply and its ability to address energy demand requirements across geographies, globally. A significant growth of global energy use in the last years has been shown¹: driven by enhanced demand across sectors such as buildings, industry and transport, the total energy supply increased 2.5 times between 1971 and 2020, and 39% in the last twenty years. In 2020, global energy use in buildings (defined as the sum of residential, commercial and public services sectors) accounted for almost 40% of the total energy use, including primary use of the energy required to produce the associated electricity and heat, generating over a quarter of human-made carbon dioxide emissions^{1,2}.

In International Energy Agency (IEA) member countries, the largest residential use of energy, all sources combined, is for heating purposes (not necessarily reflecting the global picture), followed by appliances³. In the United States, 35% of total primary energy consists of heating, ventilation and air conditioning (AC)⁴ and similar proportions are expected for China within five years. China and the United States are driving energy demand in buildings, followed by Europe for heating and India for cooling⁵. In IEA countries, space cooling may account for up to 20% of total energy and up to 30% of total electricity use in residential buildings in different countries, with shares varying mainly depending on climatic conditions and on levels of diffusion of cooling equipment, as shown in Supplementary Fig. S1 (not complete in coverage since based on a sample that actually shares end-use data with the IEA). It is also well known that most of the largest metropolitan areas are in developing countries, such as India, southeast Asia and Africa, and most of them are in warm to hot climates⁶. Following the recent increase in ownership of cooling equipment, although often still far from reaching saturation, cooling is the fastest increasing energy use in the buildings sector: it doubled its share in residential energy use in IEA countries over the last twenty years. Notably, several tropical countries with potentially high cooling requirements still have rather low percentages of households equipped with air conditioning - which implies a large potential for a significant increase of energy use in the future, as shown in Supplementary Fig. S2. IEA estimated a three-fold increase in global air conditioning stock by 2050⁷, as reported in Supplementary Fig. S3.

While the sensitivity of electricity consumption to temperature depends primarily on location, penetration of air conditioning equipment across buildings, and thermal quality of the building stock, at the first order, cooling consumption relates to outdoor air temperature. Degree days represent a measure of how much (in degrees) and for how long (in days) the outdoor air temperature is below/above a certain threshold (respectively HDD/CDD) and their trends have been used as metrics for future building energy demand^{8,9}. In short, HDD/CDD describes the overall need for warming/cooling.

Cooling degree days are defined as from formula (1)

$$CDD_b = T_e - T_b \quad (1)$$

for $T_e > T_b$, where T_e is the external temperature and T_b is the base temperature. For instance for CDD₂₁, the base temperature $T_b = 21$ °C and, given a daily time series of external average temperatures as $T_e = 18, 24, 30$ °C, the total CDD₂₁ index will result in $0 + 3 + 9 = 12$ °C.

In addition, we also consider the humidity corrected CDD, named CDD_{hum}, taking into account the perceived temperature instead of air temperature only, to have an indicator better representing the human body disease. Humid Cooling Degree Days are defined as from formula (2)

$$CDD_{hum} = TP_e - TP_b \quad (2)$$

for $TP_e > TP_b$, where TP_e is the external perceived temperature and TP_b is the base perceived temperature. The perceived temperature is computed aiming at combining the effects of air temperature and relative humidity, empirically, into a single parameter that provides a measure of the perceived temperature (more info available at <https://www.iea.org/articles/weather-for-energy-tracker>).

Spinoni et al.⁹ (2017) pointed out that population weighting of HDDs and CDDs better represent the energy load; population weighting results in lower HDD and higher CDD values when averaged over all Europe due to the low weights assigned to wide and more sparsely inhabited regions in northern Europe. On average, heating degree days are decreasing⁸ and cooling degree days are increasing⁹, and their relative contribution to the energy demand is not uniform in space. For example, Waite et al.⁴ show that among thirty-five cities analyzed worldwide, OECD (Organization for Economic Co-operation and Development) cities show a 35-90 W/°C/capita cooling electricity response to ambient air temperature changes in contrast to 2-9 W/°C/capita in non-OECD ones.

On a national level, CDDs are fundamental metrics for cooling energy demand, which is expected to grow because of expected increased penetration of cooling equipment at global scale. The changing climate will likely provide an additional driver to increase cooling demand.

Not only the annual number of CDDs can be useful for the evaluation of the tendency and the interannual variability of cooling energy demand, but also their clustering in space and time (at the high frequency, e.g., daily) matters. Wang et al.¹⁰ identified groups of US states sharing temporal patterns for CDD by a clustering algorithm and assessed sensitivity of monthly per capita residential electricity demand by means of a hierarchical Bayesian regression model for some (economic) factors such as GDP, discovering that the sensitivity to CDDs is stronger for northeastern US. A similar clustering approach was developed for the optimization of energy supply in a Brazilian city by detecting seasonal trends and anomalies like for September/October, when the demand varies between weekdays and weekend¹¹. Temperature, and CDDs in particular, are very important not only as a metric of energy consumption, but also because they affect energy supply. An important climate risk for the energy sector is represented by drought-induced cooling water shortages to thermo-electric power plants: during intense hot periods power plants are not only stressed by higher demand, but also require bigger availability of cooling water. Despite the gradual decommissioning of these plants, the coming Carbon Capture and Storage technologies are above 50% more water-intensive than conventional plants¹².

Temporal clustering of energy-related climate indices, as HDDs and CDDs, is not much investigated in the literature. But since the clustering might have an impact on the definition of the energy storage capacity and on the peak energy production capacity of a country, an additional aim of our work is to provide a first assessment of the temporal clustering of such indices, with a special focus on clusters of intense CDD, at the global scale. Research on temporal clustering in the past found evidence of extreme events that tend to cluster in alternating quiet and active periods in terms of number of events. Trends of climate indices, defined as day counts above local thresholds, exhibit symmetric changes in the cold and warm tails of the temperature distributions on long periods and asymmetric changes on shorter ones¹³, as for the case of extreme temperature over Europe in the period 1946-1999. There is also evidence for temporal clustering of extreme events during the past hurricane activity in Florida and models for yearly counts of hurricanes have been improved by determining a cluster size of two hurricanes per year¹⁴. Since

Table 1 Available variables in the IEA-CMCC dataset¹⁸.

NAME	DESCRIPTION	UNITS	AVERAGE
Temperature	Temperature (taken 2 m above ground)	°C	Population, surface
Temperature_{dew}	Dew point temperature (taken 2 m above ground))	°C	Not averaged
Temperature_{wb}	Wet bulb temperature (taken 2 m above ground))	°C	Population, surface
Precipitation	Total precipitation	mm/h	Surface
Snowfall	Snowfall	mm/h	Surface
Runoff	Runoff	mm/h	Surface
Evaporation	Evaporation	mm/h	Surface
Cloud	Cloud coverage	%	Surface
DNI	Direct normal radiation	J/m ² /h	Surface
GHI	Global horizontal irradiance	J/m ² /h	Surface
Pressure	Surface pressure	Pa	Surface
Temperature _{max}	Temperature max (taken 2 m above ground))	°C	Population, surface
Temperature _{min}	Temperature min (taken 2 m above ground))	°C	Population, surface
HeatIndex	Heat index (taken 2 m above ground))	°C	Population
Humidex	Humidex (taken 2 m above ground))	°C	Population
CDD	CDD (using a base temperature of 65 °F)	°F days	Population
CDDX	CDD (X °C, X = 10/16/18/21/23/26)	°C days	Population
CDDTholdX	CDD (X °C, X + 3 °C threshold, X = 18/21/23)	°C days	Population
CDDVar	CDD (variable)	°C days	Population
CDDhum	CDD (65 °F, humidity)	°F days, humidity	Population
CDDhumX	CDD (X °C, humidity, X = 10/16/18/21/23/26)	°C days	Population
CDDhumTholdx	CDD (X °C, X + 3 °C threshold, humidity, X = 18,21,23)	°C days	Population
CDDhumVar	CDD (variable, humidity)	°C days	Population
CDDwet	CDD (65 °F, wet bulb)	°F days	Population
HDDX	HDD (X °C, X = 14/16/18/20)	°C days	Population
HDDTholdX	HDD (X °C, X-3 °C threshold, X = 16/18/20)	°C days	Population
HDDVar	HDD (variable)	°C days	Population
HDD	HDD (using a base temperature of 65 °F)	°F days	Population
HDDwind	HDD (14 °C, wind)	°C days	Population
RH	Relative humidity	%	Surface
Daylight	Sun light	minute	Population, surface
WindXint	Wind speed (X m, X = 100/10)	m/s	Surface
WindXdir	Wind direction (X m, X = 100/10)	degree (anticlockwise, 0° East)	Not averaged
Wind100power	Wind capacity factor (100 m)	%	Not averaged

NAME indicates the variable name (bold if **primary**) in the filename, AVERAGE indicates if averaged by population or by surface for aggregated variables available at the country level. Variable is available at grid level only when "Not averaged is specified". Parameter X denotes separate variables. More detailed information is available in the User guide downloadable at: <https://www.iea.org/data-and-statistics/data-product/weather-for-energy-tracker>.

Poisson processes assume unrealistic independence among events, one approach to count rare events could be analyzing the dispersion (i.e., ratio of variance over mean of the count distribution, subtracted by one for equi-dispersion that represents the ratio of equal variance and mean), that for positive values indicates possible clustering since the over-dispersion supports the time aggregation of events. For example, a north-south pattern for clustering of extra-tropical cyclones in western Europe has been highlighted¹⁵. A peak over threshold quantile-based approach can be also considered to analyse the peak of electricity demand on a daily basis^{16–19}.

Understanding trends in CDDs, as well as the distribution and trends of the occurrence of their extreme events, at global and national scales, provides an essential basis to the analysis and planning of the potential evolution of cooling energy demand in buildings, globally. The present work aims to provide a global assessment of trends of national level CDDs, and a first assessment of their time clustering, based on a new dataset of energy-related climate indicators made available by the International Energy Agency (IEA, <https://www.iea.org/>) and the euro-Mediterranean Center on Climate Change (CMCC, www.cmcc.it). This dataset²⁰ is based on ERA5 reanalysis (<https://www.ecmwf.int/en/forecasts/datasets/reanalysis-datasets/era5>) and includes a number of indicators (Table 1) that are relevant to analyse energy supply and energy demand, both at grid and national level. In the database, demand-related indicators such as CDDs, are defined according to

several thresholds and averaged nationally, either by surface or by population weight, in order to better represent the national energy consumption profiles (see the Data and Method section).

Next section describes our results, both in terms of trends of national CDDs and on their clustering in time, with focus on those (tropical) emerging countries that are more exposed and less adaptive to thermal stress. We calculate specific parameters to represent the aggregation in time of consecutive intense days and investigate their tendencies from the first (2000–2009) to the last (2011–2020) decade of the past period, for selected countries. We include both results from standard dry CDDs and humidity-corrected CDDs (CDDhum) over the same regions.

Results

Humidity-corrected Cooling Degree Days. We are interested in countries with high cooling demand, which is driven by high temperature and humidity. For this purpose, among the available indicators we selected humidity-corrected cooling degree days at 21 °C threshold, CDDhum21. The importance to consider the humidity factor in determining stress conditions for the human body, leading to a more pronounced request of cooling, is also made evident in Fig. 1: most of the tropical countries are affected by increasing CDDhum21 (Fig. 1, panel b), even more than dry CDD21 (Fig. 1, panel a). Many of the most affected countries are also densely populated (India, Bangladesh, Thailand among others) and subject to a not negligible population increase in the

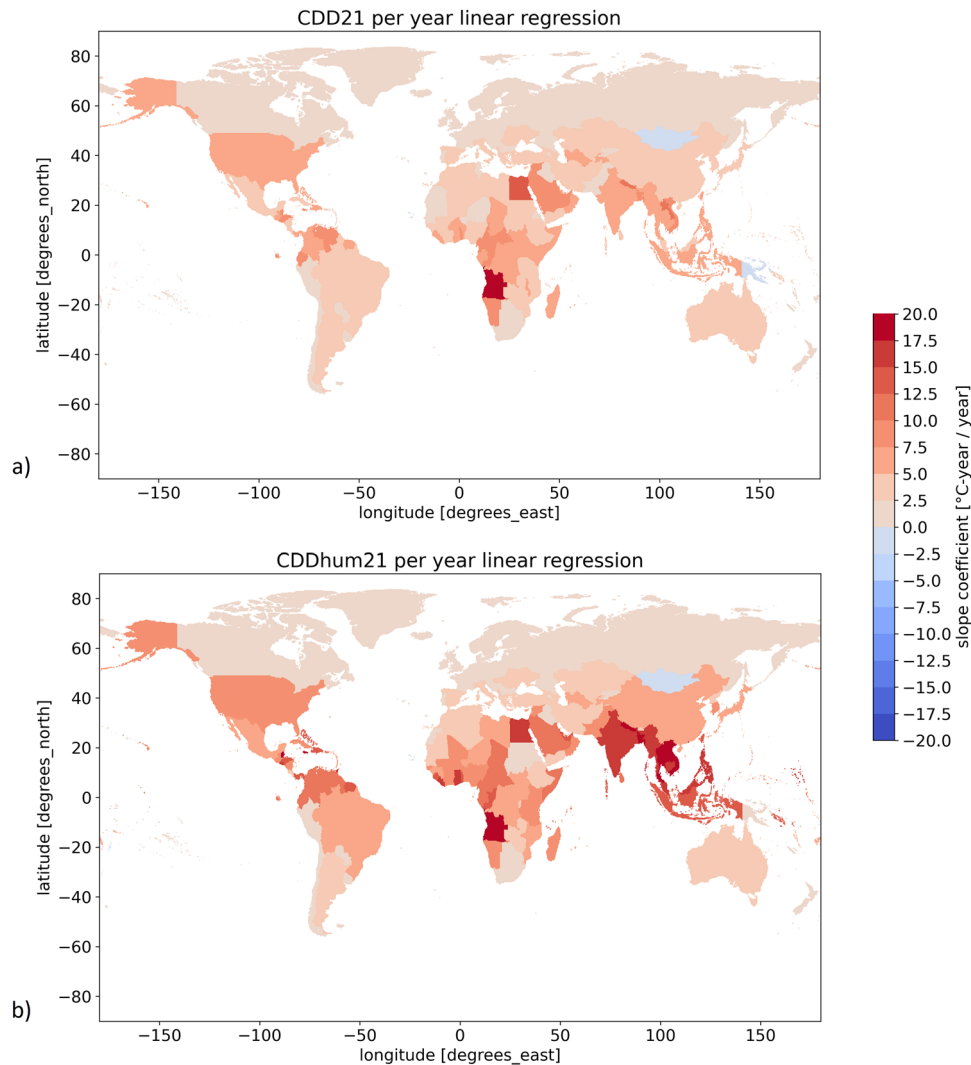


Fig. 1 Global trends of national-level CDD21 and CDDhum21, based on IEA-CMCC (2022) over the period 2000-2021. CDD21 is shown in **a**. CDDhum21 is shown in **b**.

considered period, reinforcing the value to consider indices weighted based on the population distribution (see methods). A first look into CDDhum21 nationally aggregated values shows a rising tendency in the frequency, particularly in the temporal clustering, of intense days (days when the daily CDDhum21 value exceeds the 90p value of the whole CDDhum21 series, see Methodology) worldwide. In fact, the majority of available regions (see Supplementary Table S1) have significantly higher values in the second decade for the selected parameters (see Methods). For example, the total number of intense days (N) per decade rises in almost all countries. In terms of clustering, at least one of the considered parameters rises in more or less 75% of the considered countries and 50% of the countries shows all parameters rising. We know that both frequency and temporal clustering of intense days induce greater cooling energy demands and the countries affected by such significant increases are mainly concentrated in South America, Southeast Asia and Africa. In the sample there are also less developed countries for which it is more difficult to cope with higher cooling energy demand. The effect in the distribution of intense CDDhum21 days is measurable worldwide, and thanks to this updated dataset (<https://www.iea.org/articles/weather-for-energy-tracker>) we will keep track of next changes in the CDDhum21 spatio-temporal distribution.

By classifying countries according to the national 75p of CDDhum21 over the two decades (considering the warm season only, see Methods) the top 23 countries (representing the top 10%) are mainly located in the tropics with Central Africa, Arabic Peninsula and South Asia leading. Figures 2 and 3 show the linear regression of CDD and CDDhum21 per year (see Methodology) for the four countries, within the selected 23, showing the most pronounced increase in the trend of the annual accumulated values: Fig. 3 shows that the CDDhum21 per year has risen the most in Bangladesh (Fig. 3 panel a) with $22.31^{\circ}\text{C}\cdot\text{year}$ per year until 2020, meaning that the necessity of cooling increased considerably in intensity and duration. High positive trends are also found for Thailand (Fig. 3 panel c) and India (Fig. 3, panel d). There is concern for Bahrain (Fig. 3, panel b) since this is the country with the highest CDDhum21 values that also increased, in the twenty years considered, from about 3200 to 3600 $^{\circ}\text{C}\cdot\text{year}$. Following this trend, the impact on the national energy supply could worsen fast in the the near future.

Countries of Arabic peninsula dominate when considering the temporal variability expressed in terms of standard deviation (SD). In fact, the greatest values of standard deviation (SD) are found in Bahrain, Qatar and Iraq, followed by Hong Kong and Pakistan (Fig. 4). The spatial pattern of intense CDDhum21 values, expressed as the 90p, over each country (Fig. 5) suggests

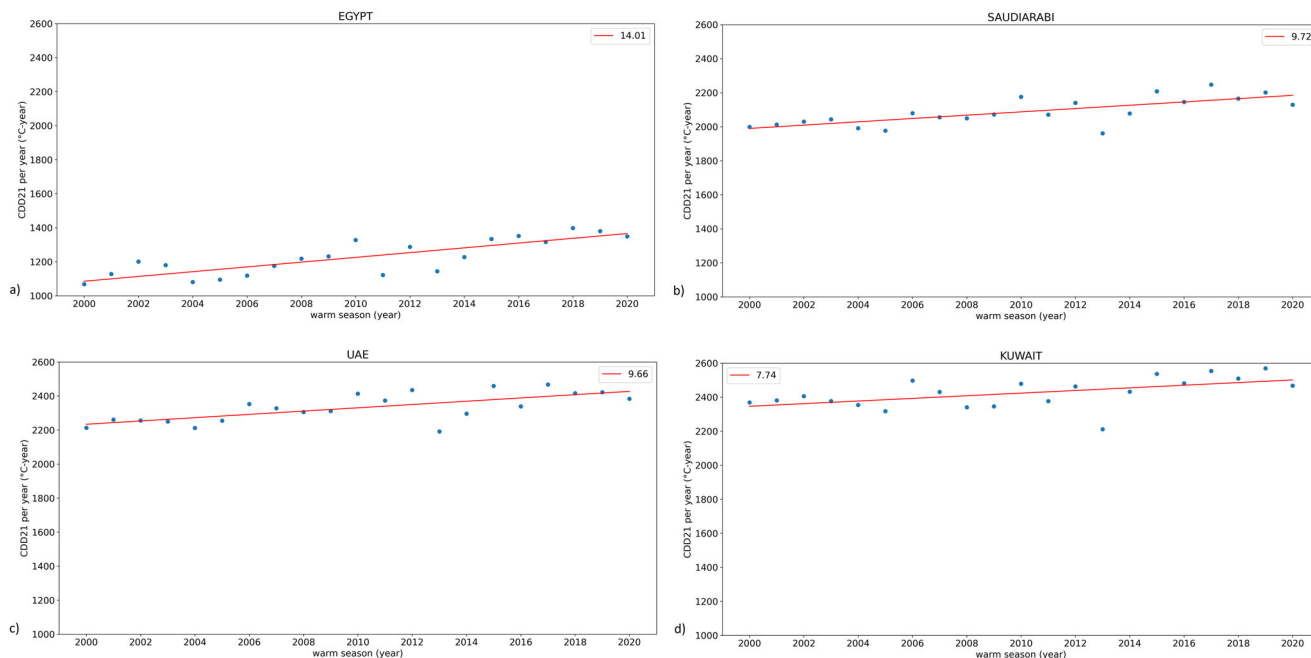


Fig. 2 Linear regressions of yearly CDD21-accumulated (warm season only) for top four countries according to the coefficient, significant at the 5% level. Egypt, Saudi Arabia, United Arab Emirates and Kuwait are shown in **a**, **b**, **c** and **d** respectively.

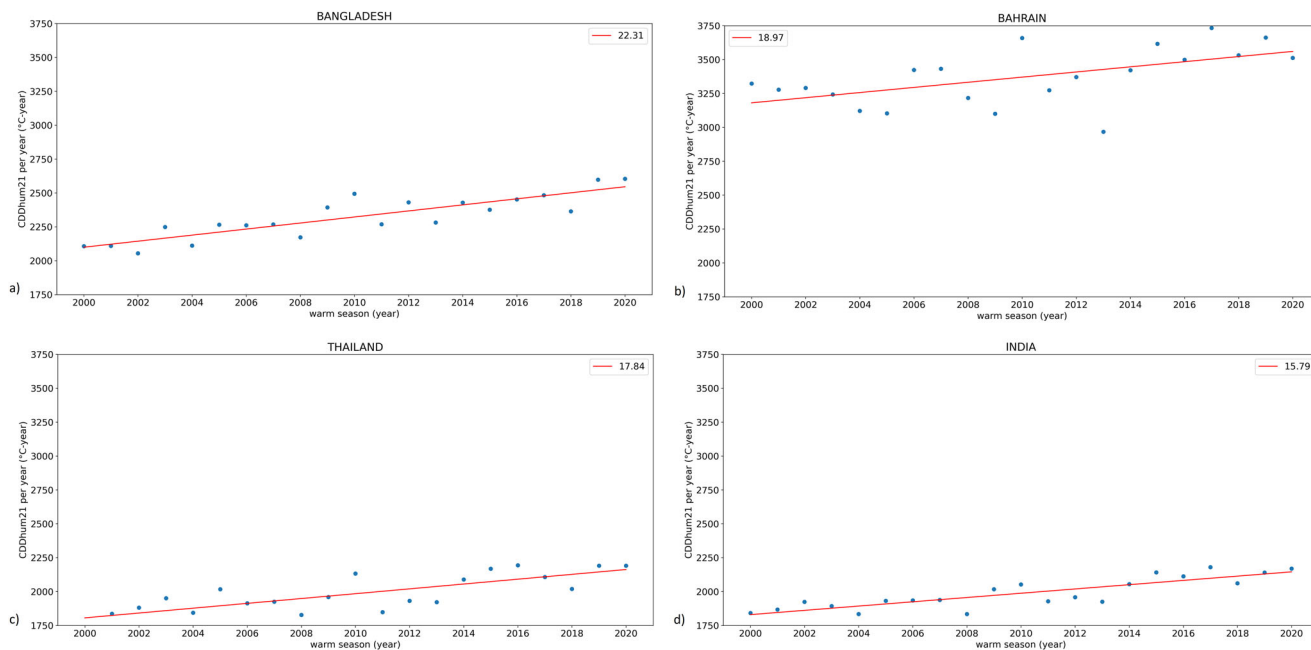


Fig. 3 Linear regressions of yearly CDDhum21-accumulated (warm season only) for four top countries according to the coefficient, significant at the 5% level. Bangladesh, Bahrain, Thailand and India are shown in **a**, **b**, **c** and **d** respectively.

highest values for the tropical countries of the Northern Hemisphere (all of the 23 highlighted countries are located in the Northern Hemisphere) such as United Arab Emirates, Kuwait, Iraq, Pakistan, Saudi Arabia and Bangladesh, followed by India, Vietnam, Cambodia, Thailand, Mali, Mauritania and Niger.

Figure 6 presents the CDDhum21 time series for a selected set of countries from this group: Bahrain, Iraq, Hong Kong, Pakistan respectively in panels a,b,c,d. Looking at the peaks indicated by the intense days when the percentile threshold (blue line in Fig. 6) is crossed, the magnitude shows little variability in time. On the

other hand, peaks look wider in the second half, and we observe a tendency of increasing clustering of intense days especially for 2016 and 2017 years in those countries. This apparent regularity will be investigated to check for temporal clustering (Table 2).

A higher cooling needs are expected in the second decade as intense periods last longer because of increased clustering (Fig. 6, red marks), in Hong Kong especially. Computing the cumulated CDDhum21 over the year, an increasing tendency is found for all of the 23 regions. These trends are everywhere significant (5% level) except for six countries in the subset. Looking at the yearly trends of the total cumulated values of CDDhum21 over the full

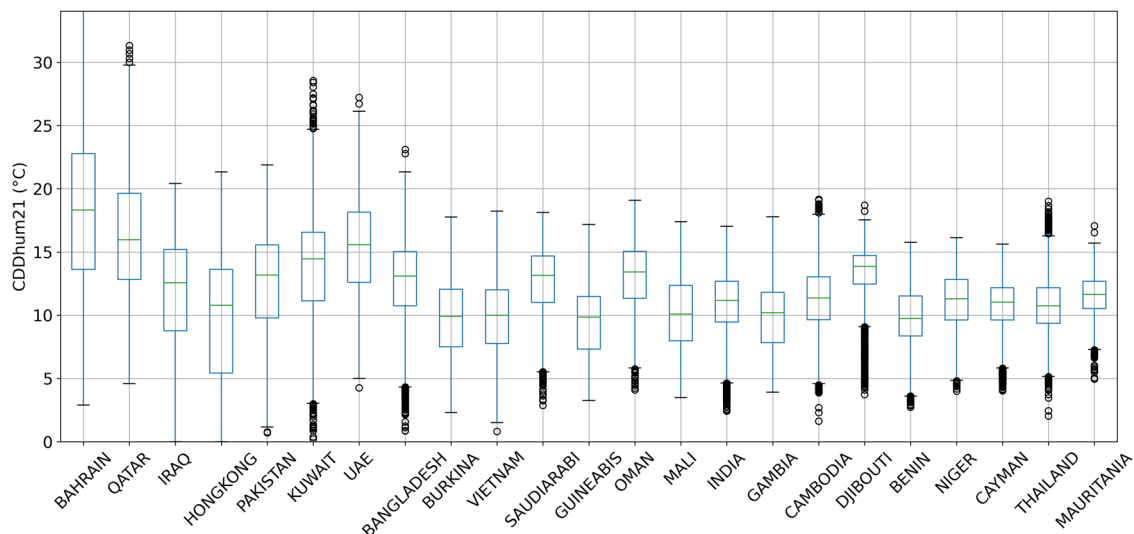


Fig. 4 Distribution of CDDhum21 for the first decile of countries (23) with highest 75th percentile. Countries are sorted by decreasing standard deviation of CDDhum21. In these box plots the blue rectangle indicates the interquartile range (IQR), the green line the median, the whiskers extend to $Q1-1.5 * IQR$ and $Q3 + 1.5 * IQR$ or to the last data point if it is less than this value. Any points that fall beyond the whisker limits (black dash) are known as outliers (black circles).

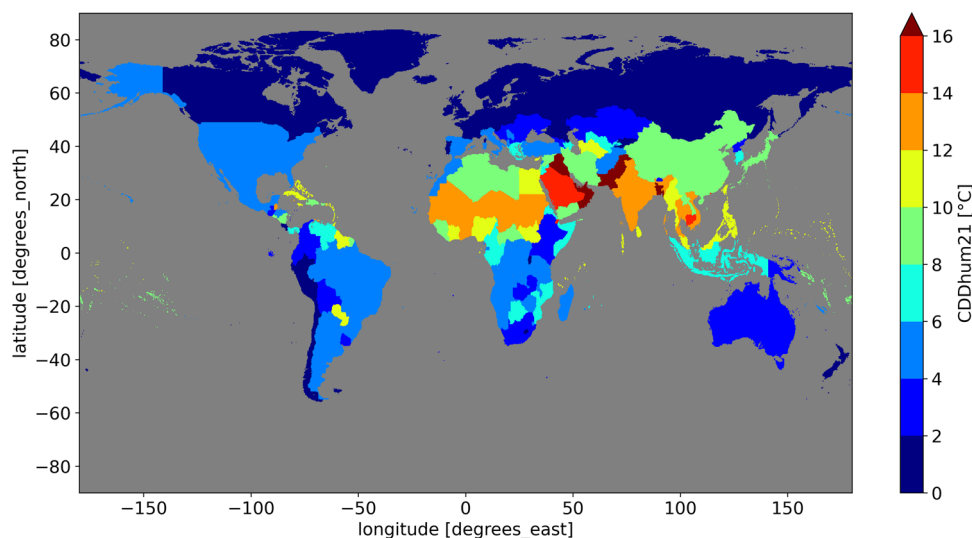


Fig. 5 Map of regions by their 90th percentile value of daily CDDhum21 over 2000-2020. Warm season only is shown as MJJASO/NDJFMA according to the latitude.

period, different countries emerge by their slope coefficient. These locations are also characterized by important growth of the urbanization degree over 2000-2020.

The results relative to the clustering of CDDhum21, based on the computation of the Coefficient of Variation (see Methods), are summarized in Table 2: the top twenty-three countries are located in the northern hemisphere, concentrated in Arabia and South East Asia. Table 3, instead, shows the 75th and 90th percentiles, and other statistical parameters for CDDhum21 (see Methods) computed over the whole 2000-2020 period. The total number of intense days (N) increase significantly everywhere moving from the first to the second decade of the considered period, except for Iraq where it slightly decreases from 190 to 178. The strongest increase of N, from 70 in 2000-2009, to 298 in 2011-2020 is observed in Thailand. In general, the total number of intense days almost doubles from the first to the second decade, but a threefold increase is found for Vietnam, India, Bangladesh and Cambodia. This means that high-end cooling

demand is rapidly increasing in already warm countries affecting severely the population and challenging the energy grid in richer countries. Bahrain leads both in magnitude and variability, with a high value for the coefficient of variation (CV) suggesting the tendency to clustering. Over the 20 years period all the countries show values of CV greater than two and some greater than four, such as Burkina Faso, Mali and Benin. This gives evidence for clustering of intense CDDhum21 days in these regions. The change of CV from the first to the second decade is significant for most countries. Despite the increase of N, in Bangladesh, the CV is almost the same. On the other hand, CV strongly increases in Cambodia, Burkina Faso, Mali, Niger, India, Thailand and Vietnam (where it raised from 1.89 to 3.33). Looking at the distribution of the intense days, several clusters of (at least 2) consecutive days arise. To characterize the clustering motivated by the CV values we compared the decade 2000-2009 against the decade 2011-2020 through the total number of clusters and their maximum size in the decade. In Table 2 the temporal clustering is

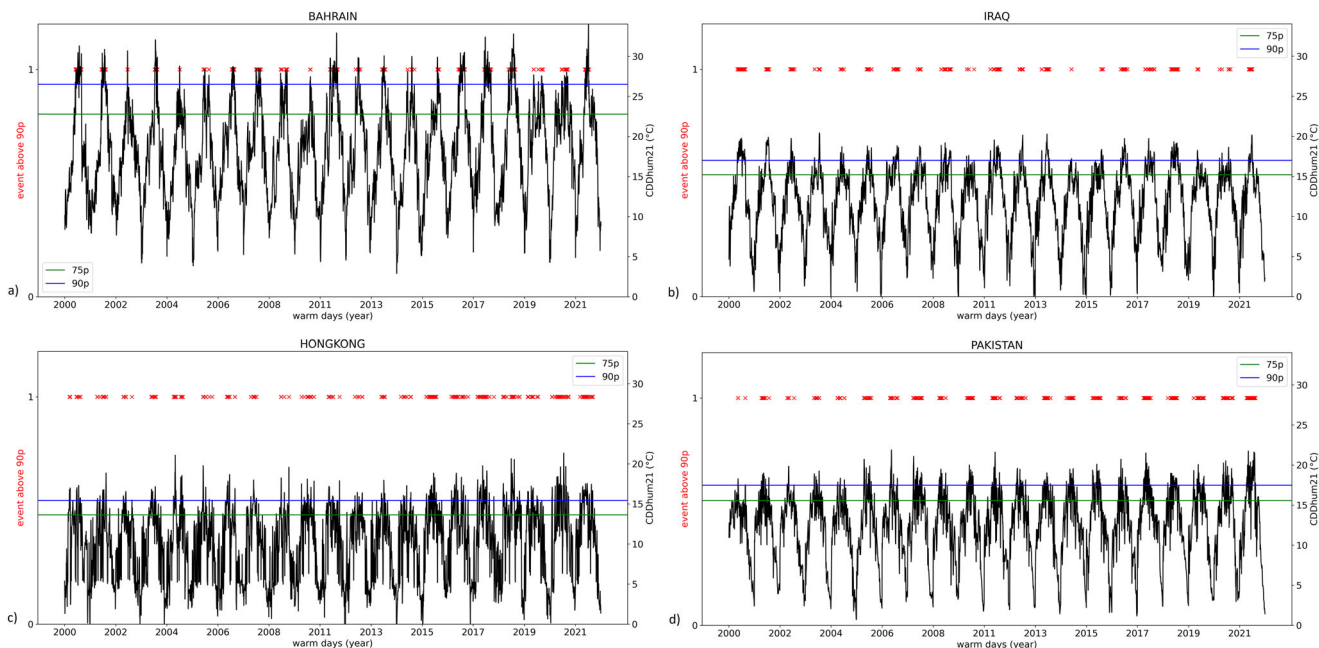


Fig. 6 Time series of CDDhum21. In black the CDDhum21 and the associated point processes, as red crosses (only days above threshold) for the top four countries. The thresholds of 75th percentile and 90th percentile (which is used for the point process) are indicated respectively in green and blue. Bahrain, Iraq, Hong Kong and Pakistan are shown in **a**, **b**, **c** and **d** respectively.

Table 2 CDDhum21 values of the 23 countries sorted by decreasing standard deviation, separately for the decade 2000–2009 (I in table) and the decade 2011–2020 (II).

Country	CV I	CV II	K I	K II	N I	N II	N_C I	N_C II	M_C I	M_C II
BAHRAIN	2.83	3.21	11.13	12.36	150	218	25	33	18	25
QATAR	2.80	3.00	8.95	9.76	160	208	33	46	13	23
IRAQ	2.91	2.94	10.92	9.61	190	178	28	32	29	22
HONG KONG (China)	2.06	2.87	4.19	7.51	115	253	29	58	9	15
PAKISTAN	2.41	3.21	5.09	8.26	129	239	35	59	6	19
KUWAIT	2.49	2.96	8.59	10.40	125	243	25	41	14	17
UNITED ARAB EMIRATES	2.68	2.92	7.09	8.71	159	209	38	43	9	17
BANGLADESH	2.26	2.31	4.32	5.69	94	274	21	71	8	11
BURKINA FASO	3.71	4.72	7.87	8.76	126	242	30	69	8	8
VIET NAM	1.89	3.33	2.28	7.94	79	289	22	60	5	11
SAUDI ARABIA	2.51	3.27	9.00	12.14	122	246	23	32	15	49
GUINEA-BISSAU	2.75	3.08	5.88	6.67	149	219	35	50	13	9
OMAN	2.52	3.31	7.31	10.12	125	243	22	46	26	20
MALI	3.47	4.53	6.80	8.60	123	245	30	63	8	12
INDIA	2.61	4.13	8.15	11.07	80	288	13	47	12	23
GAMBIA	3.15	3.50	5.50	8.20	167	201	43	43	7	13
CAMBODIA	2.95	3.95	5.32	9.73	97	271	18	50	9	16
DJIBOUTI	2.18	3.06	5.28	7.02	149	219	29	46	9	13
BENIN	3.53	4.43	9.61	9.59	135	227	24	50	20	13
NIGER	2.94	4.27	5.55	8.56	106	262	24	61	12	11
CAYMAN ISLANDS	2.30	3.10	5.05	7.36	126	242	31	57	7	9
THAILAND	2.71	4.25	4.80	9.90	70	298	17	57	9	23
MAURITANIA	2.37	2.44	3.49	4.96	157	211	42	60	4	7

For each country the coefficient of variation CV, the K function, the total number N of events above 90p, the total number of clustered events N_C and the maximum cluster size M_C in days of the decade (in bold countries where differences are 5% statistically significant) are shown.

expressed also in terms of the K function (see Methods). The K function of Bahrain, Kuwait, Saudi Arabia, Oman and India exceeds ten days in the second decade, while in Thailand and Vietnam is more than doubled. These former countries, in fact, show a significant clustering in time for the other parameters too. The increase of the K function from the first to the second decade is significant for most countries, similarly to CV. In Mauritania

and Bangladesh the K function raises significantly, despite the CV does not follow the same tendency.

In general, the last decade exhibits a general strong increase both in the occurrence and the duration of clusters, suggesting a potential increase in the cooling demand as well as a more clustered demand, less sparse in time, inducing persistent stress conditions for people and energy providers.

Table 3 75th and 90th percentiles of the the region aggregated CDDhum21 time series.

Country	75p	90p	SD	CV	K
BAHRAIN	22.79	26.51	5.93	3.05	11.71
QATAR	19.65	23.86	4.93	2.94	9.44
IRAQ	15.2	17.00	4.42	2.91	10.15
HONG KONG (China)	13.63	15.44	4.41	2.53	6.40
PAKISTAN	15.56	17.47	4.34	2.84	7.12
KUWAIT	16.57	18.10	3.97	2.87	9.52
UNITED ARAB EMIRATES	18.15	20.27	3.87	2.81	8.04
BANGLADESH	15.03	16.78	3.55	2.63	5.23
BURKINA FASO	12.06	13.89	3.07	4.32	8.52
VIET NAM	12.01	13.52	2.86	2.99	6.93
SAUDI ARABIA	14.68	15.84	2.80	2.94	11.25
GUINEA-BISSAU	11.49	12.72	2.79	3.02	6.77
OMAN	15.06	16.09	2.74	2.99	9.25
MALI	12.37	13.87	2.73	4.09	8.10
INDIA	12.69	13.91	2.70	3.73	10.31
GAMBIA	11.82	13.19	2.62	3.28	6.79
CAMBODIA	13.03	14.32	2.62	3.74	9.05
DJIBOUTI	14.73	15.37	2.43	2.6	6.20
BENIN	11.53	12.79	2.30	4.03	9.50
NIGER	12.83	13.86	2.25	3.83	8.06
CAYMAN ISLANDS	12.18	13.01	2.23	2.78	6.32
THAILAND	12.19	13.51	2.20	3.89	9.46
MAURITANIA	12.69	13.66	1.62	2.41	4.37

The Standard Deviation (SD), the Coefficient of Variation (CV) and the Ripley's K function (K) (see Methods) of intense days for the full period 2000-2020 (warm season only) are also shown.

Sixteen countries show an increase in the size of the maximum cluster (M_C , see Methods) from the first to the second decade. M_C doubles in Vietnam and Thailand, while three times greater values are found for Pakistan and Saudi Arabia (where M_C moved from 15 to 49). Furthermore Saudi Arabia, together with Bahrain, United Arab Emirates and Gambia (all countries with larger M_C in the second decade), are the countries where the number of clustered intense events per decade (N_C) didn't increase significantly. On the other hand, over most of the other countries the total number N_C of clusters doubles in the second decade. In particular, moving from the first to the second decade, 22 clusters became 60 in Vietnam, 13 clusters became 47 in India, 17 clusters became 57 in Thailand and 21 clusters became 71 in Bangladesh. A significant increase of N_C as well as M_C is found in the last four countries. These countries are the most interesting since they show significant values for all the three parameters. In other words, in Vietnam, India, Niger and Thailand not only the intense days have risen in the last decade but also their clustering in time, implying higher and more concentrated in time energy demand. Figure 7 focuses on the results over these countries. Starting from N_C yearly series (Fig. 7, red lines) we notice a clear positive tendency. The decade 2000-2009 is characterized by lower N_C values, in fact there are also years with few to absent clusters like 2000, 2001, 2002 and 2008 especially in India and Thailand. The variability of N_C through the years is high in Thailand and Vietnam where the maximum value of 12 clusters in 2020 is reached. Furthermore, Thailand's variability arises also for M_C (Fig. 7, panel d). The yearly widest cluster size exceeds 20 days with the exceptional 24 days long cluster of 2010 in Thailand. Instead, India exhibits a more regular positive tendency for both N_C and M_C (Fig. 7, panel b).

Moving from the aggregated point of view (Table 2) to the grid point (see Methods), the results summarized in Table 4 are, in

general, confirmed. Regarding the N parameter, both magnitudes and trends are similar, suggesting that the two methods could be considered equivalent (aggregation does not change the outcome). The countries most demanding for cooling energy with N exceeding 150 days in the first decade are Qatar, Iraq, United Arab Emirates (UAE hereafter), Oman and Gambia. Instead, considering a higher threshold of 250 day in the second decade the high demanding countries are Hong Kong, Bangladesh, Vietnam, Cambodia and Thailand (Table 2 and Table 4). An interesting difference is given by Iraq where the detected decreasing trend of N, obtained based on aggregated data, results increasing when moving to the grid point approach. The number N_C of clustered events is the indicator better preserved between the two methods, especially in the case of Qatar, Hong Kong and Cambodia. Generally the differences shown in Table 4 well agree with the ones shown in Table 2, also when the magnitudes are different, such as in the case of Pakistan and Kuwait. For Iraq and Gambia the found increases are more pronounced compared to aggregated results (Table 2). The potential demand for energy is significantly higher in the second decade, according to most of the significant countries in Table 2, showing the same increase and the same magnitude in Table 4, except for Pakistan and India where also other indicators are less preserved. This is suggesting that, possibly, the population distribution in this region has an important effect and this will be the object of future investigation. Interesting to note that differences for clustering in the two decades over Qatar, are significant only when computed on aggregated values (Table 2) and not when computed at the grid point level and then aggregated (Table 4).

Dry Cooling Degree Days. Figure 1 shows that the extended CDD rising tendency along the tropical belt is confirmed for CDD21 (Fig. 1, panel a) with pattern similar to the CDDhum21 (Fig. 1, panel b) but with a lower magnitude. This is confirmed by Supplementary Table S2, compared to Supplementary Table S1. The frequency of intense days has risen worldwide and the temporal clustering too. Greater values of the selected parameters in the second decade are found in most of the regions. The number of countries affected by significant changes in the clustering is of the same order of magnitude but slightly smaller when humidity is removed (Supplementary Table S2 with respect to Supplementary Table S1). The four parameters together changed in 87 countries, where both frequency and temporal clustering of intense days are driving higher energy demand for cooling. These countries are concentrated in South America, Southeast Asia and Africa, where population is also increasing meaning that cooling will be an even higher key issue related to energy demand. Again, the notable cases of e.g., U.S.A. and Spain are present, recalling that the effect in the distribution of intense CDD21 days does not involve only less developed regions. Similarly to what has been done for CDDhum21, from now on the top 23 countries, based on the intensity of CDD21 daily values, are investigated, since these are the regions with potentially strong consequences for people's health and where cooling energy demand could grow dramatically. The shown increase in CDD21 is consistent with previous works suggesting a significant change over all continental areas. This is consistent with the already highlighted climate-driven energy demand trends for heating and cooling, more pronounced moving from pre-1990 to post 1990²⁰.

Neglecting humidity, the results for CDD21 are similar both in terms of magnitude and clustering, but generally less pronounced. Additional countries such as Turkmenistan, Egypt, Chad, South Sudan and Togo appear in the list (Table 5 to be compared to Table 2). However, the order based on decreasing SD is changed and some countries are no more statistically significant in terms

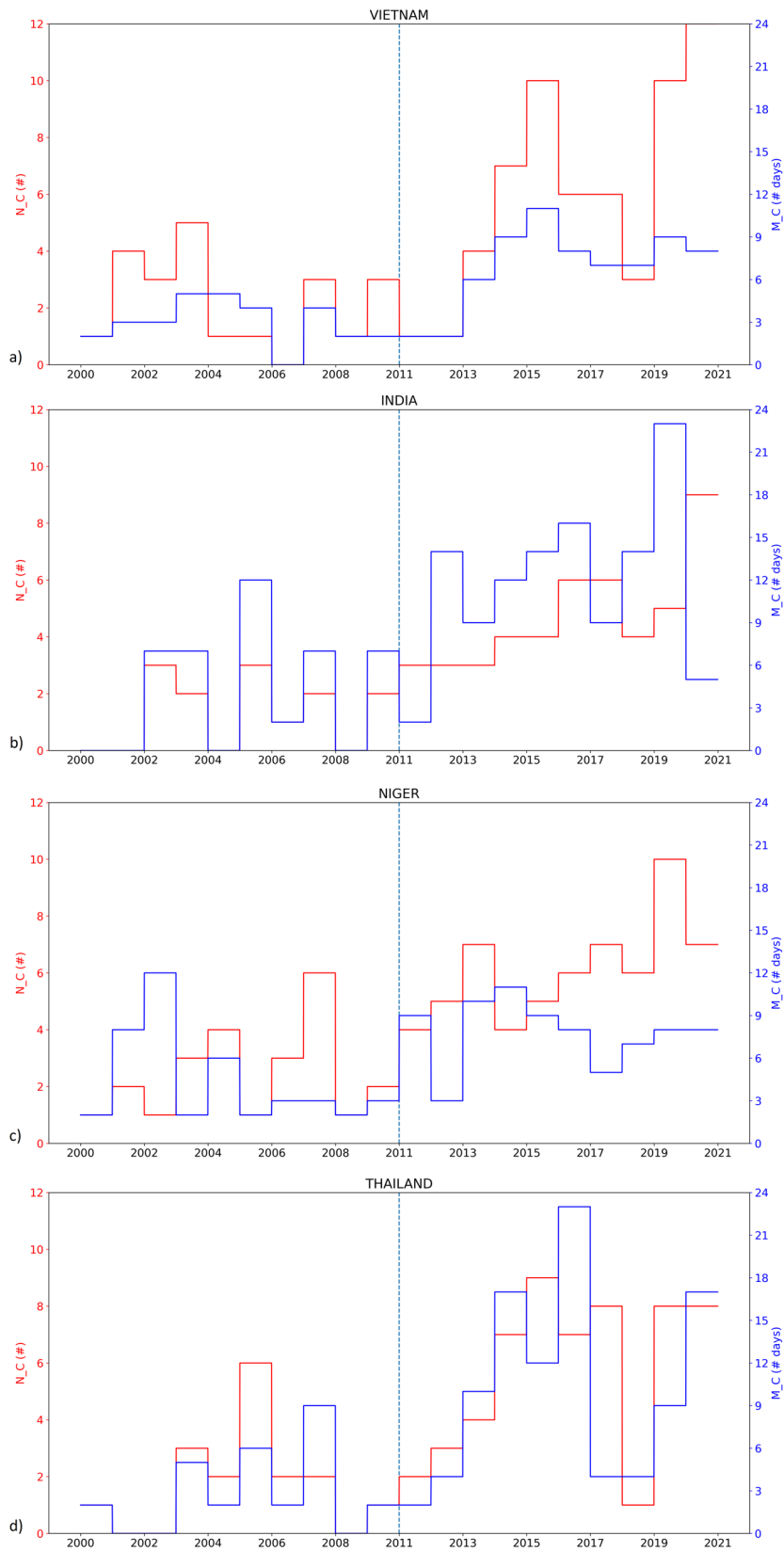


Fig. 7 Number of clustered CDDhum21 events and size of the maximum cluster. N_C is shown in red and M_C (units are days) is shown in blue. Annual values are shown, for the countries where both indicators are significant at the 5% level. The dashed line separates the decades and represent the removal of 2010 year. Vietnam, India, Niger and Thailand are shown in **a**, **b**, **c** and **d** respectively.

Table 4 Analogous of Table 2 where N, N_C and M_C are the averages of the same indicators, calculated for each grid point inside the nation, weighted by the corresponding gridded population.

Country	N I	N II	N_C I	N_C II	M_C I	M_C II
BAHRAIN	142,05	206,72	25,97	29,13	18,97	24,79
QATAR	154,97	199,85	34,03	42,33	14,18	22,54
IRAQ	175,02	182,72	33,84	36,19	18,51	18,54
HONG KONG (China)	118,41	257,27	28,48	55,33	9,03	17,52
PAKISTAN	136,12	221,77	34,34	52,28	7,99	13,99
KUWAIT	130,12	227,67	29,42	53,98	13,67	15,8
UNITED ARAB EMIRATES	156,86	210,61	36,56	44,71	9,87	15,25
BANGLADESH	100,94	264,99	22,11	66,61	9,14	11,33
BURKINA	126,38	228,42	30,39	61,99	8,47	8,12
VIET NAM	91,14	262,63	20,94	54,23	7,87	17,52
SAUDI ARABIA	125,15	225,01	27,71	46,11	11,65	17,6
GUINEA-BISSAU	146,3	205,54	34,34	46,06	11,43	12,84
OMAN	154,02	209,3	35,85	44,9	12,85	15,23
MALI	121,01	233,46	30,27	58,7	6,82	10,83
INDIA	121,92	236,38	26,83	45,97	12,22	19,66
GAMBIA	162,78	201,96	38,42	43,11	8,61	12,25
CAMBODIA	85,97	260,16	17,84	50,98	8,73	21,36
DJIBOUTI	130,94	234,16	28,87	53,3	7,99	13,26
BENIN	144,11	215,91	35,28	51,22	10,33	11,36
NIGER	106,72	240,69	22,96	59,75	8,73	9,31
CAYMAN ISLANDS	121,77	230,59	29,91	57,04	7,14	7,27
THAILAND	90,31	251,74	20,46	51,27	7,64	15,99
MAURITANIA	131,68	225,85	28,9	52,69	8,29	10,35

The countries where all parameters changed significantly from I to II decade are highlighted in bold.

Table 5 Same as Table 2 but for CDD21 instead of CDDhum21.

Country	CV I	CV II	K I	K II	N I	N II	N_C I	N_C II	M_C I	M_C II
IRAQ	2.90	2.94	10.85	9.61	190	178	28	32	29	22
TURKMENISTAN	2.44	3.22	5.09	9.10	132	236	32	46	10	23
KUWAIT	2.33	3.05	5.48	7.72	128	240	36	65	7	10
BURKINA FASO	3.94	4.46	7.82	9.57	154	208	33	40	14	15
PAKISTAN	3.40	3.48	6.70	7.72	169	199	39	40	13	9
UNITED ARAB EMIRATES	2.29	3.17	5.79	10.59	105	263	24	41	8	25
SAUDI ARABIA	1.88	3.53	4.68	11.59	73	295	18	41	9	37
EGYPT	2.06	2.81	4.07	7.78	108	260	26	46	7	26
MALI	4.21	4.36	9.78	9.58	164	204	37	39	15	12
QATAR	2.66	2.86	5.17	7.05	161	207	44	53	6	11
NIGER	3.84	4.54	8.08	9.12	150	218	30	48	14	13
CHAD	3.72	4.75	10.17	10.75	138	229	22	44	16	15
DJIBOUTI	2.69	3.03	5.72	9.45	148	220	32	41	8	13
BAHRAIN	2.74	2.86	7.20	7.43	161	207	38	49	8	16
OMAN	2.97	3.35	5.95	7.45	130	238	30	54	8	13
INDIA	3.70	4.43	11.15	11.70	149	219	21	30	39	30
SOUTH SUDAN	3.13	3.55	7.54	9.97	157	205	30	37	13	16
SUDAN	3.80	4.32	8.50	9.20	155	213	34	43	13	20
MAURITANIA	2.96	3.18	5.28	6.57	159	209	42	55	10	13
BANGLADESH	2.55	2.30	5.04	5.22	123	245	25	65	13	9
BENIN	3.44	4.11	9.60	10.14	144	218	27	43	21	14
TOGO	3.14	3.96	8.40	9.53	134	228	28	41	20	12
CAMBODIA	3.08	3.79	6.82	9.61	124	244	25	42	10	16

of N_C and M_C changes, such as Burkina and India with poor evidence for clustering tendency. The opposite is valid for Bahrain and Saudi Arabia where clustering is now statistically significant for both N_C and M_C. In Fig. 8 the global pattern of intense CDD21 is shown: the map is similar to the one shown for CDDhum21 (Fig. 5) with less pronounced values especially over the tropics.

In the case of dry CDD21 the strongest trends of cumulative potential cooling energy demand, displayed in Fig. 2, are found in

Egypt (14.01 °C-year/year) followed by Saudi Arabia, UAE and Kuwait (7.74 °C-year/year). The much higher tendency of Egypt is interesting and further analyses could verify how the degree of urbanization has changed during the considered twenty years as well.

Table 5 also contains the results of the K function in the dry case over the two decades (for the statistical values computed over the whole 2000–2020 period please refer to Table 6). The highest values above ten days in the second decade are found in UAE,

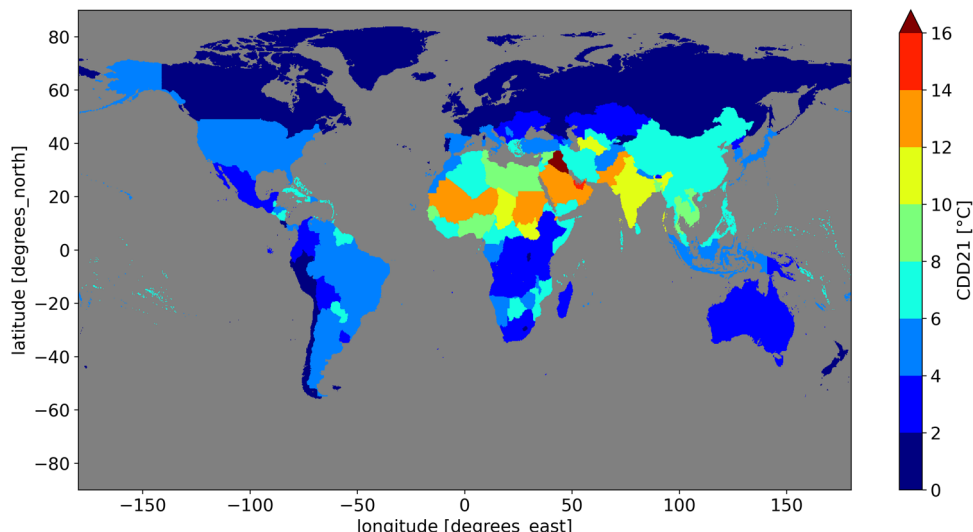


Fig. 8 Map of regions by their 90th percentile value of daily CDD21 over 2000-2020. Warm season only is shown as MJJASO/NDJFMA according to the latitude.

Table 6 The CDD21 results analogous to Table 3.

Country	75p	90p	SD	CV	K
IRAQ	15.2	16.99	4.42	2.94	10.21
TURKMENISTAN	9.04	11.03	4.17	2.86	7.60
KUWAIT	16	17.16	3.64	2.72	6.79
BURKINA FASO	10.77	12.33	3.26	4.21	8.69
PAKISTAN	11.13	12.53	2.80	3.43	7.16
UNITED ARAB EMIRATES	14.57	15.65	2.55	2.85	9.10
SAUDI ARABIA	13.25	13.99	2.52	2.93	10.25
EGYPT	8.53	9.43	2.51	2.54	6.51
MALI	10.02	12.32	2.47	4.29	9.68
QATAR	14.34	15.29	2.44	2.75	6.22
NIGER	11.17	12.98	2.36	4.23	8.91
CHAD	8.87	11.11	2.26	4.27	10.67
DJIBOUTI	12.23	13.02	2.25	2.92	8.03
BAHRAIN	12.58	13.42	2.22	2.81	7.26
OMAN	12.57	13.59	2.15	3.27	6.88
INDIA	8.85	10.60	1.98	4.14	11.89
SOUTH SUDAN	9.75	10.91	1.94	3.32	8.77
SUDAN	10.76	12.16	1.91	4.06	8.82
MAURITANIA	11.01	12.11	1.62	3.12	6.20
BANGLADESH	8.3	9.03	1.37	2.64	5.06
BENIN	8.31	9.01	1.30	3.8	9.85
TOGO	8.16	8.82	1.28	3.6	9.10
CAMBODIA	7.96	8.74	1.23	3.53	8.97

Chad, Benin as well as in India and Saudi Arabia. In particular, removing the effect of humidity, the K function more than doubles in Saudi Arabia. The majority of countries show a significant rise in the K function for the second decade, in agreement with the CV, except for Iraq, Mali, Bahrain and Bangladesh. Similarly to CDDhum21, also for CDD21, the K function looks to better represent the temporal clustering in this context.

N_C (and N) of dry CDD significantly increased from 2000–2009 to 2011–2020 for most of the countries. Among the most affected regions the increase of all parameters is more pronounced in Saudi Arabia. It is remarkable that moisture affects not only the geographical pattern of intense days but also their clustering in time. In fact, M_C difference is statistically significant for CDD21hum in 70% of the 23 countries, while for CDDhum21 only for 56%. There are some countries with higher

evidence in the tendency for clustered cooling demand, having N_C changes significant for both humid and dry cases: this is the case of Niger, Oman and Bangladesh.

Figure 9 shows the analysis of clustering for the three relevant regions of UAE, Saudi Arabia and Oman. Regarding the number of clustered CDD21 events (N_C), the increase in cluster density from the first to the second decade is evident (red line). It is important to highlight the high temporal variability in Oman, when in the year 2012 the maximum number of 9 clusters is found, followed by the 2013 year associated to no clusters at all. In support of a more intense second decade, all of the three regions share big values of N_C, where also UAE reaches 9 clusters. Looking at the blue line in Fig. 9, relative to the size of the maximum cluster (M_C), the variability results higher for UAE and Saudi Arabia where maximum cluster size exceeds 20 days in 2012 and 2017. Comparing Fig. 9 with Fig. 7, we notice that humid countries have more, but smaller, clusters than dry ones with the record of 37 consecutive intense days in 2017 for Saudi Arabia.

In Table 7 the results at the grid point level are shown. Similarly to what we found for the humid case, the magnitudes and the increasing trends agree with those of the aggregated counterpart (Table 5). Iraq, Burkina, Pakistan, Mali, Qatar, Bahrain, South Sudan, Sudan and Benin are the countries potentially most demanding for cooling energy with N exceeding 150 days in the first decade. The second decade's threshold of 250 day is crossed only by Egypt in the humid case (Table 5) but a significant increase up to 235 is found also in the dry case (Table 7) confirming the Egypt as the most affected country in the last decade. The general equivalence in the two approaches is confirmed, with the exception of Iraq in accordance with Table 7. In Supplementary Table S1, covering all of the countries, the N_C is the better preserved indicator, especially in terms of magnitude in the second decade.

The agreement of the results relative to N_C obtained based on the computation of the index based on the two methods for both CDD21 and CDDhum21, suggests that weighting for the population before or after the computation of the index is not influential for this parameter confirming that the usage of pre-computed indices, aggregated and made available on the IEA web site, is a valid approach to study the evolution of cooling energy demand for stakeholders. The maximum cluster size M_C generally agrees both in magnitude and trend, despite few

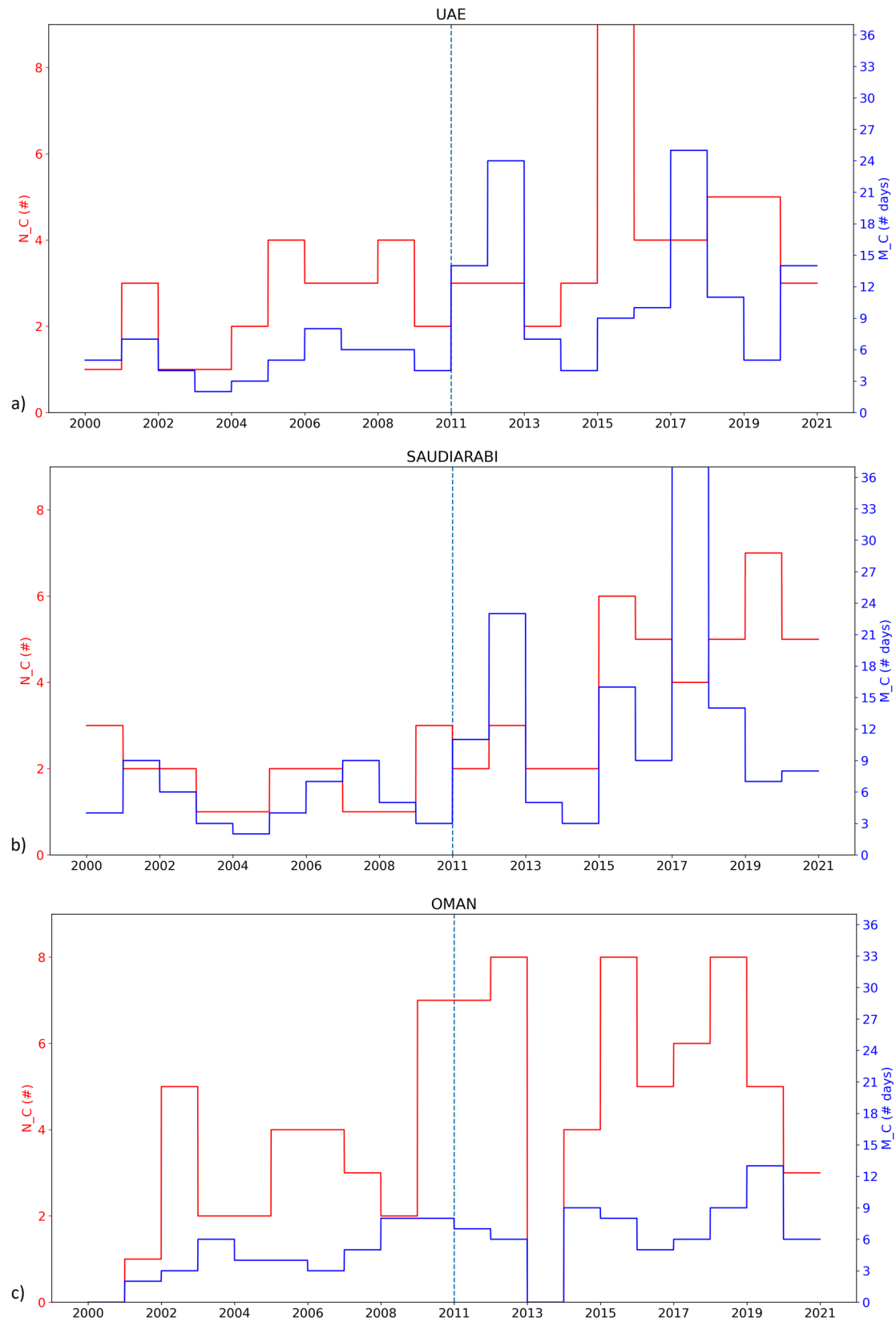


Fig. 9 The number of clustered CDD21 events and size of the maximum cluster. N_C is shown in red and M_C (units are days) is shown in blue. Annual values are shown, for the countries where both indicators are significant at the 5% level, where the dashed line separates the decades and represent the removal of 2010 year. United Arab Emirates, Saudi Arabia and Oman are shown in **a**, **b** and **c** respectively.

Table 7 The CDD21 analogous of Table 4 where N, N_C and M_C are the averages of the same indicators, calculated for each grid point inside the nation, weighted by the corresponding gridded population.

Country	N I	N II	N_C I	N_C II	M_C I	M_C II
IRAQ	175,04	182,60	33,89	36,09	18,47	18,53
TURKMENISTAN	135,80	228,42	32,96	44,40	8,15	21,34
KUWAIT	131,62	233,65	32,77	59,68	6,94	10,50
BURKINA	170,14	198,25	36,13	43,54	14,26	12,56
PAKISTAN	167,71	188,87	37,79	40,80	11,75	14,09
UNITED ARAB EMIRATES	110,70	244,65	28,57	51,38	7,32	19,08
SAUDI ARABIA	118,67	235,14	28,10	49,17	9,62	16,63
EGYPT	103,74	250,28	23,78	52,96	8,44	19,70
MALI	160,69	206,61	36,69	45,59	12,40	12,70
QATAR	157,91	211,46	42,43	53,55	7,09	10,07
NIGER	145,84	215,34	32,25	46,74	13,51	12,55
CHAD	140,21	219,81	24,22	42,91	18,16	15,29
DJIBOUTI	148,53	231,08	34,78	46,52	9,67	16,68
BAHRAIN	157,16	205,94	39,42	48,66	7,88	15,55
OMAN	156,32	216,82	35,94	50,41	10,39	12,03
INDIA	147,51	209,06	25,78	34,63	18,89	24,17
SOUTH SUDAN	174,31	192,92	31,76	41,53	15,71	14,53
SUDAN	158,93	202,79	33,47	43,47	14,14	13,98
MAURITANIA	142,52	220,08	36,85	54,06	8,38	11,57
BANGLADESH	123,77	241,72	27,11	58,23	10,89	11,35
BENIN	154,52	208,48	35,55	47,73	12,86	10,78
TOGO	147,74	212,97	34,17	50,37	11,03	12,29
CAMBODIA	109,61	244,75	21,85	45,12	10,42	20,32

The countries where all parameters changed significantly from I to II decade are highlighted in bold.

countries such as UAE, Saudi Arabia and Egypt have values of M_C in Table 7 that slightly underestimate those of Table 5. This means that not only space aggregated N, but also space aggregated M_C results, can be considered comparable using the two methods. About statistical significance, the countries agree well also for CDD21, confirming the comparability between the two aggregation methods. It is curious to note that in terms of CDD21 changes, Bahrain results now significant, while Djibouti and Oman are no more significant in all three parameters compared to CDDhum21 results.

Conclusions

This work mainly focuses on the global recent tendencies in terms of energy demand by emerging countries for cooling needs. The energy demand is here expressed in terms of Cooling Degree Days, both standard (CDD) and humidity-corrected Cooling Degree Days (CDDhum), weighted by population, based on a joint IEA-CMCC database (<https://www.iea.org/articles/weather-for-energy-tracker>). The database derives country level indicators at global scale from the year 2000 and is regularly updated at the country level with quarterly frequency. Few studies make use of population weighting for CDD⁹, and even less studies consider humidity, which is relevant to characterize heat stress conditions²¹. The aim of this work is to fill this gap based on actual data rather than projections, especially for emerging countries, for which there are no studies on this subject.

First, we show that cooling degree days have increased significantly worldwide. Then we found that intense events showed increased tendency to cluster in a set of countries with high cooling demand. We also demonstrate that considering humidity is relevant, compared to the standard CDD, highlighting the importance to use a proper measure of (a country's) levels of warmth.

The concept of energy reliability for peak demand is important for energy providers' planning. This is often based on the

distribution of 90th percentile (the threshold for intensity of cooling degree days applied in our study, see Methods) of past high temperatures assuming a stationary climate²². Here we show that significant changes in the clusters emerge between the last two decades for specific tropical countries.

Most of the high demanding countries, according to CDDhum21 are located in Asia led by the Arabic Peninsula (Bahrain at the top). Looking at the yearly accumulated values, over the considered twenty-year period, the positive significant trend is observed almost everywhere, with countries in the tropical belt showing a trend ranging from about 15 to about 25 °C-year/year (see Fig. 1). Similarly, the distribution of intense days is asymmetric towards the last decade for most of the countries. In particular, India and Thailand become warmer, and also register an increase of the number and length of intense events, together with Vietnam and Niger. On the other hand, Thailand shows a less clear tendency given the high temporal variability of N_C and M_C.

In the first decade of the current century the total energy demand of Vietnam more than doubled²¹. A relevant cause is the fast population rise, particularly true for the urbanized one. Our findings confirm positive trends in the buildings' cooling potential demand, but also that demand becomes more clustered with longer intense periods. Today Vietnam is self-sufficient in the energy supply, however it is expected to import energy soon. On this respect the government had proposed several energy efficiency and conservation policies to control the impact of near future energy demand. A study on world largest metropolitan areas⁶, reported the cities of Madras (India), Bangkok (Thailand) and Ho Chi Minh (Vietnam) as the warmest ones looking at annual CDD, followed by many other Indian cities. They observed that given the rising electrification rate as well as AC penetration the Mumbai city alone has a potential future cooling demand that corresponds to the 24% of the current demand in the entire US (in population-weighted CDD). We confirm this positive trend, and we add that not only more clusters are

emerging but also their duration tends to be longer, meaning that their estimate could be conservative if clustering is ignored. In Bangkok (Thailand) the already highlighted warming trend²³ is in line with our results up to 2012 and we show that it continues until now.

The consequences of the described tendencies in Niger can be even worse, considering that it struggles meeting the low daily energy demand, often resulting in summer shortages. Most of the electricity consumption (a total of 474 GWh in 2010²⁴) comes from the capital city of Niamey and Niger imports more than 85% of its energy from Nigeria. We stress that the harsh conditions will be exacerbated by shortages due to significantly more frequent intense periods, for the last decade, in the order of 6 clustered events per year (10 only in 2019) with mean length of 7 consecutive days, as reported in Table 2. Several simulations agree that future cooling demand will be led by Indonesia, China and particularly India where the impact of rising CDD is more pronounced²⁴ in agreement with our evidence and reaching 60% of the peak summer load. Today 8% of Indian households have air conditioning and are expected to grow six-fold in the next twenty years. A survey in Delhi (highest electricity consuming region in India) suggested that above 40% of households own AC²⁵. The growing demand for AC in India, driven by higher incomes, will stress the energy grid under longer clusters as shown in this paper. Our results suggest that considering CDD instead of CDDhum in India might hide the clustering effect that is not negligible (Table 2 for details).

Removing the effect of humidity gives notable differences. In fact, some countries, such as Hong Kong, emerge only when humidity is considered, or when it is neglected, such as Egypt. But more surprising is the effect on temporal clustering, where Saudi Arabia shows an increase in clusters only on dry conditions. On the other hand, the clustering over India is significant only on humid conditions. In the dry climate UAE, Saudi Arabia and Oman are the only regions where clusters increase significantly both in number and length. Instead, Kuwait, Bangladesh and especially Niger are relevant in both dry and humid analysis, hence requiring more awareness on health and energy standpoints. In Saudi Arabia the population raised by 2% but the energy demand raised by almost 5% per year²⁶. Figure 9 shows that the clusters notably increased in the last 20 years in Saudi Arabia and a single cluster can overcome an entire month as in 2017. UAE is one of the highest energy consumers per capita in the world because of its economic and population growth and a low cost for energy²⁷. Over 1980–2000 the electricity consumption for cooling raised from 5 to 50 billion kWh. We found that UAE has a tendency in clustering similar to that of Saudi Arabia, with very long clusters which stress energy supply for longer. Despite the strong increase in clusters, these Arabian countries could mitigate the consequences by financing an energy-efficient transition of the emerging residential sector that is more effective under their drier climate.

The results of Table 4 for CDDhum21 and Table 7 for CDD21 show that the prior aggregation in space, used to provide the IEA dataset available online (<https://www.iea.org/articles/weather-for-energy-tracker>), is not a limiting factor for the temporal analysis here presented. The results obtained for N, N_C and M_C are similar and confirm a strong increase of the cooling energy demand. In this sense N_C is the least affected by the method of aggregation and can be used for the statistical analysis of cooling energy demand based on the already aggregated data. For some countries, in the CDDhum21 case, the increase of M_C is different between the two approaches and bigger in the original countries' aggregated dataset linked to different magnitudes of M_C in the first decade. This is unclear and it could be motivated by some regional factors, not investigated in the present work.

Finally, the results found in Table 4 and Table 7 largely confirm those of Table 2 and Table 5 respectively, so we consider the input dataset suitable for temporal analysis of CDDhum21 and CDD21. For a better interpretation of the clustering results, Tables 2 and 3 are partially summarized in Fig. 10, where the clear geographical pattern for the temporal clustering of the significant changes in CDD indices emerges.

In general, in the selected countries the increase in cooling demand overwhelms the slight decrease in heating demand (not shown) resulting in an overall rise in energy demand in the last two decades, stronger in 2011–2020. In addition, the energy consumption is not limited only by households' income but also by energy access. Evidence from India suggests that, differently from urban areas, in rural areas energy poor (i.e., low-end consumers) households are 57% where only 22% are income poor²⁸. This means that if economic development will improve energy access, the increase in the energy demand can exceed the supply, resulting in more summer shortages, already more frequent in Southeast Asia because of the earlier discussed CDDhum21 clustering.

Based on our analysis, intense population-weighted humidity-corrected cooling degree days have significantly increased during the considered twenty-year period in 14 countries out of the sample of 23, 9 of them only when humidity is considered. Humidity is important also for clustering and intensity. India, Cambodia, Thailand and Vietnam are the emerging countries where this effect is stronger. Further studies should consider these regions, where a large part of global population lives, to assess the impacts on the future energy sector. The metric used for estimating heat exposure here reflects the need for the adoption of air conditioning, already increased dramatically worldwide as average temperature increases²⁹ and this need might become even more pressing in the future depending on the radiative scenario³⁰.

Methods

Reference data. To explore the impacts of weather and climate on the energy sector, IEA jointly with CMCC developed a series of energy-related climate indicators based on ERA5 reanalysis³¹, covering the period 2000–2022 and made it available online³². The horizontal resolution is 0.25° of longitude-latitude and the temporal resolution ranges from daily to yearly. Data are available at the grid level and at the country aggregated level for a total of 234 countries. Data are available in different formats as netCDF files, Excel files, and customized extractions from the visual platform are also available. Each indicator is provided at the global scale, for a total of 10 primary indicators and 42 derived indicators (see Table 1). In general, variables at the country level are derived based on averaged over grids weighted by surface, if primary, or weighted by population if derived, though few variables are available for both averaging methods. Primary indicators are weather variables such as mean temperature and precipitation that serve to calculate derived indicators such as CDD and HDD. The population data are derived from the dataset of gridded population at 0.25° spatial resolution from NASA SEDAC³³, including population estimates consistent with national censuses of 2000, 2005, 2010, 2015, 2020, and linearly interpolated for the years in-between. In particular, CDD time series are available at 10, 16, 18, 21, 23, 26 °C base temperatures and represent the cumulated differences of mean daily temperature above these fixed thresholds. The humidity-corrected CDD time series are based on the same thresholds (now on CDDhumX with X = 21 °C in our study), and reflect the fact that human thermal comfort is affected by moisture, better representing the cooling demand especially for tropical countries. This work uses CDDs and CDDhum based on the threshold of 21 °C, and averaged nationally, based on population weights, to more accurately relate to buildings energy demand.

Methodology. To identify the optimal timespan for the annual warm period, we compared different six-month periods' averages across all countries and decided to define the *warm season* as the periods May to October (MJJASO) and November to April (NDJFMA), for the countries located in the Northern and Southern Hemisphere, respectively. Exploring different thermal thresholds and statistical indicators, we ended choosing the criterium of 75th percentile (75p) of daily CDDhum21 values from 2000 to 2020 limited to the warm season, to determine the countries to focus on, for cooling demand tendencies and clustering. The same ranking is obtained using the 90th (90p) percentile. Also, the usage of different temperature thresholds (X value) in the computation of the CDDhumX index - such as X = 21,

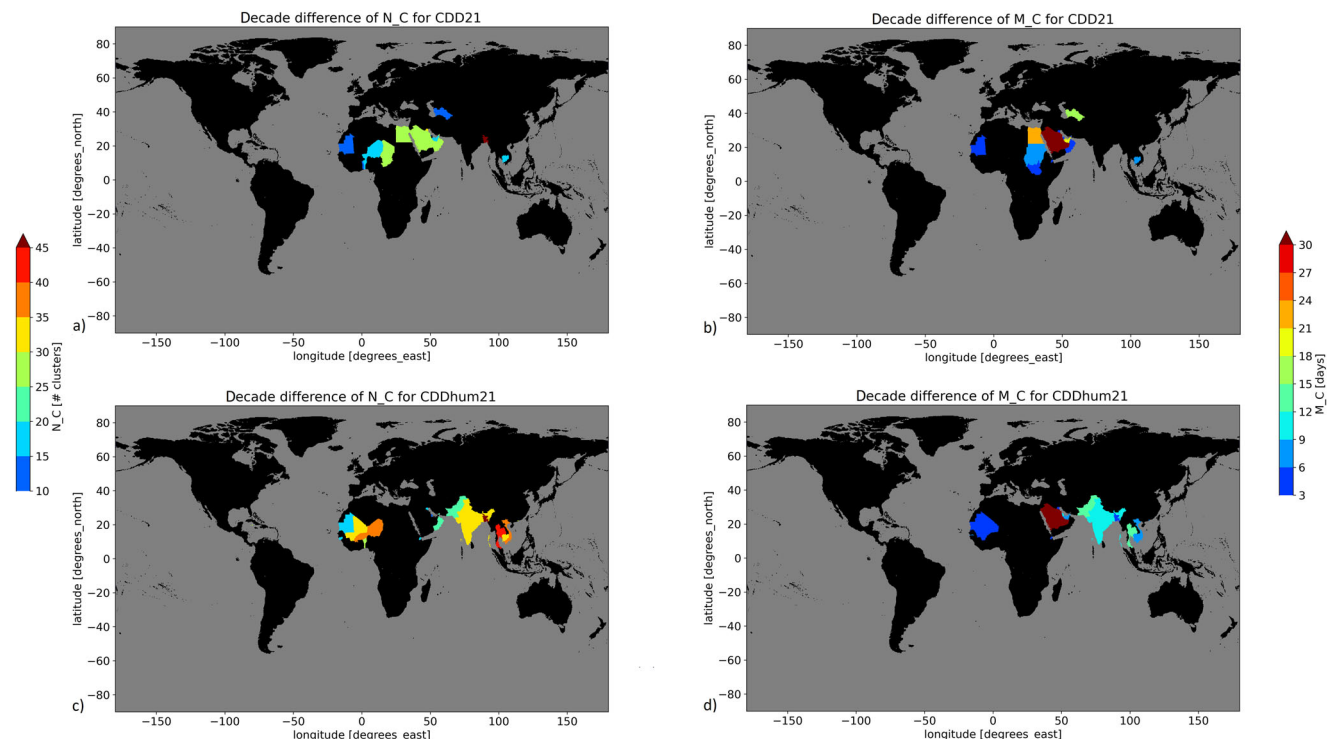


Fig. 10 CDD21 and CDDhum21 changes in the second decade compared to the first decade. Differences of indicators N_C (a and c) and M_C (b and d) from the first decade to the second, both for CDD21 (a and b) and CDDhum21 (c and d), are shown as calculated in Table 2 and Table 5 for countries where the difference results statistically significant. Black color is associated to all the remaining countries.

23 and 26 °C – leads to the selection of the same countries: there is no dependence on this threshold in the definition of the top decile of the warmth countries.

We first analyze the temporal tendencies of total cooling demand by means of CDDhum21 per year and CDD21 per year (measured in °C-year and obtained by summing the daily series of CDD over the year, in our case limited to the warm season MJJASO) to identify countries affected by most pronounced tendencies: to assess total (relative to warm season) CDD-driven potential cooling demand, we performed a linear regression of yearly cumulated values of CDDhum21 and CDD21 at global scale (see Fig. 1). Cumulated CDD are often used to study tendencies of potential cooling demand^{6,34}. Linear regressions here are related to cumulated CDD measured as °C-year (as in Figs. 2 and 3) while the rest of the paper refers to °C-day unless otherwise specified.

Then, we focus on areas of potentially intense cooling demand analysing the temporal clustering of daily CDDhum21 (and CDD21). Boxplots are also used to represent the distribution of CDDhum21 events (Fig. 4). We first determine all countries worldwide showing any increase in the indices related to temporal clustering, as reported in Table S1 for CDDhum21 and Table S2 for CDD21. The temporal clustering is mainly considered for the evaluation of the number of clustered intense events per decade (N_C) and the number of days of the widest cluster per decade (M_C). Then we focus on the countries where CDDhum21 75p values result higher (driving a more relevant energy demand for cooling), selecting the top decile: in other words we ranked the countries based on the 75p value resulting from CDDhum21 time series in each country and we selected only the top decile. This results in a sub-set of twenty-three countries (Fig. 4), all showing statistically significant results in terms of tendency in temporal clustering. Important to note that the ranking results the same using the 90p threshold instead of the 75p: the countries top decile does not change.

To observe the distribution in time of intense CDDhum21 daily values over the 2000–2020 warm season, and to analyze the clustering in time, we set a threshold of 90p (different values are associated to different regions) for daily CDDhum21 (and CDD21), and defined a binary time series consisting of values 1 when the daily CDD is above the threshold (i.e. intense days) and values 0 when it is below³⁵. We count the number of intense events in each year, the duration of each event, and the distance in days between each intense event and the following one. Based on the prior binary series we define series of inter-event times, times in days spanning between an event (intense day 1-valued) and the following, by counting consecutive 0-valued not intense days; in case of consecutive intense days the difference is set to 0 (e.g. starting from a series [1 0 0 1 0 1] we get [0 3 0 1 0] where zeros correspond to previous ones and positive numbers correspond to aggregated count of previous zeros). We can calculate the Coefficient of Variation (CV) of this series checking for values above 1 (the threshold of a not clustered process), as the ratio of standard deviation over mean, equal to 1 for events evenly distributed

(equidispersed) in time³⁶. We look for clustering as overdispersion (i.e., $CV > 1$), meaning that standard deviation of time differences is greater than the mean difference and consequently more events are distributed as clusters in time. In addition to the CV defined over the entire 20 years period, we also provide CV computed over decades to highlight changes from the first to the second decade (Tables 2 and 5): decade I covers the period 2000–2009, decade II covers the period 2011–2020.

We define clusters as the groups of (at least two) consecutive intense days (above the 90p threshold). The size of the cluster represents its duration in days and higher values indicate a longer driver for cooling energy demand. The maximum duration of clusters is studied for trends over the two decades, comparing specific parameters across the two decades 2000–2009 and 2011–2020, and testing for significant differences, given the relatively short period covered by the dataset. Through a simple random sampling with replacement bootstrap (simple bootstrap) method, 95% confidence intervals are defined for the differences in the means before and after 2010. The parameters analyzed (Tables 2 and 5) are: N as the number of intense days per decade, N_C as the number of clustered intense events per decade and M_C as the number of days of the widest cluster per decade. While Tables 2 and 5 show the results only for the top-23 countries, for completeness the results are extended worldwide in Supplementary Tables S1 and S2, respectively, for all region where a 5% statistically significant difference between decades is found for at least one parameter, independently of the magnitude of degree days values.

A similar analysis is performed at the grid point level: from the CDDhum21 time series, the same indicators described above are calculated for each grid point within a given country ($0.25^\circ \times 0.25^\circ$ longitude by latitude grid). Every single point is characterized by a specific time series of CDDhum21/CDD21 that is analyzed by first calculating the grid point's temporal 90th percentile necessary to compute the three indicators. After the calculations of N, N_C and M_C, those are averaged with the corresponding decade's average of interpolated population data within the region. In other terms, here we calculated the indicators at each grid point and only then we averaged them over the population, while in the former approach the indicators were calculated at the national level from the already population-weighted cooling degree days, in order to answer if prior averaging of variables³¹ (IEA-CMCC, 2020) could affect the clustering analysis results. The results can be found in Table 4 for CDDhum21, and this analysis is extended to CDD21 as well (see Table 7) and presented in the next section.

Another method we use to detect temporal clustering is the Ripley's K function³⁷ as defined by Barton et al. (2016): this function represents the average number of intense days within a time t (where we selected $t = 10$ days). To find a proper time window t of the K function for all countries, the resulting K function is compared to the K function retrieved from a Monte Carlo simulation of a homogeneous Poisson

process (where its intensity rate matches the average monthly number of intense days) which represents a sequence of intense events equi-dispersed in time. For each intense day we calculate the number of intense days within 10 days around that day, sum these numbers over all the n intense days and divide by n . These calculations are repeated for each of the 23 warmest countries for CDDhum21 (Table 3) and CDD21 (Table 6). Making use of the bootstrapping method, we look for statistically significant differences between the two decades in the selected countries for these parameters as well (see Table 2 and Table 5).

Since we found limited evidence in literature for clustering in time, related to degree days, we considered more than one method to generalize our results. CV and K function are better known metrics in clustering's literature but we also developed the indicators N_C and M_C to provide an alternative approach to clustering, that we consider more intuitive for the interpretation of the results.

Data availability

Data used in this work are available through the IEA - CMCC International Energy Agency, Weather for energy tracker (<https://www.iaea.org/articles/weather-for-energy-tracker>) and can be also derived, following the described methodology, based on ERA5 climate data and NASA gridded population data (<https://doi.org/10.7927/H4JW8BX5>). Table S1 doi is <https://doi.org/10.5281/zenodo.7965869>. Table S2 doi is <https://doi.org/10.5281/zenodo.7966287>.

Received: 16 December 2022; Accepted: 2 June 2023;

Published online: 13 June 2023

References

1. IEA - International Energy Agency, World energy balances. (<https://www.iaea.org/data-and-statistics/data-product/world-energy-balances>), (2022a).
2. IEA - International Energy Agency, GHG emissions from energy. (<https://www.iaea.org/data-and-statistics/data-product/greenhouse-gas-emissions-from-energy>), (2022b).
3. IEA - International Energy Agency, Energy efficiency indicators. 2022c (<https://www.iaea.org/data-and-statistics/data-product/energy-efficiency-indicators>), (2022c).
4. Waite, M. et al. Global trends in urban electricity demands for cooling and heating. *Energy* **127**, 786–802 (2017).
5. Sachs, J., Moya, D., Giarola, S. & Hawkes, A. Clustered spatially and temporally resolved global heat and cooling energy demand in the residential sector. *Appl. Energy* **250**, 48–62 (2019).
6. Sivak, M. Potential energy demand for cooling in the 50 largest metropolitan areas of the world: Implications for developing countries. *Energy Policy* **37**, 1382–1384 (2009).
7. IEA - International Energy Agency. *The future of cooling*. (International Energy Agency, 2019)
8. Shen, Liu B. & Zhou, D. Spatiotemporal changes in the length and heating degree days of the heating period in Northeast China. *Meteorol. Appl.* **24**, 135–141 (2016).
9. Spinoni, J. et al. Changes of heating and cooling degree-days in Europe from 1981 to 2100. *Int. J. Climatol.* **38**, 191–208 (2017).
10. Wang, S., Sun, X. & Lall, U. A hierarchical Bayesian regression model for predicting summer residential electricity demand across the USA *Energy* **140**, 601–611 (2017).
11. Conti, D. & Servidone, G. Discovering and labelling of temporal granularity patterns in electric power demand with a Brazilian case study. *Pesquisa Operacional* **36**, 575–595 (2016).
12. Byers, E. A., Coxon, G., Freer, J. & Hall, J. W. Drought and climate change impacts on cooling water shortages and electricity prices in Great Britain. *Nat. Commun.* **11**, 2239 (2020).
13. Klein Tank, A. M. G. & Können, G. P. Trends in Indices of Daily Temperature and Precipitation Extremes in Europe 1946–99. *J. Climate* **16**, 22–3680 (2003).
14. Jagger, T. H. & Elsner, J. B. Hurricane Clusters in the Vicinity of Florida. *J. Appl. Meteorol. Climatol.* **51**, 5–877 (2012).
15. Economou, T. Serial clustering of extratropical cyclones in a multi-model ensemble of historical and future simulations. *Q. J. R. Meteorol. Soc.* **141**, 693–3087 (2015).
16. Sigauke, C., Verster, A. & Chikobvu, D. Extreme daily increases in peak electricity demand: Tail-quantile estimation. *Energy Policy* **53**, 90–96 (2013).
17. Sigauke, C. & Bere, A. Modelling non-stationary time series using a peaks over threshold distribution with time varying covariates and threshold: An application to peak electricity demand. *Energy* **119**, 152–166 (2017).
18. Boano-Danquah, J., Sigauke, C. & Kuei, K. A., Analysis of Extreme Peak Loads Using Point Processes: An Application Using South African Data. *IEEE Access* **8**, 146105–146115 (2020).
19. IEA - International Energy Agency, Weather for energy tracker. (2020) (<https://www.iaea.org/articles/weather-for-energy-tracker>)
20. Deroubaix, A. et al. Large uncertainties in trends of energy demand for heating and cooling under climate change. *Nat. Commun.* **12**, 5197 (2021).
21. Scoccimarro, E., Fogli, P.G. & Gualdi, S., The role of humidity in determining perceived temperature extremes scenarios in Europe. *Environ. Res. Lett.* <https://doi.org/10.1088/1748-9326/aa8cdd> (2017).
22. Burillo, D., Chester, M. V., Ruddell, B. & Johnson, N. Electricity demand planning forecasts should consider climate non-stationarity to maintain reserve margins during heat waves. *Appl. Energy* **206**, 67–277 (2017).
23. Arifwidodo, S. & Chandrasiri, O. Urban Heat Island and Household Energy Consumption in Bangkok, Thailand. *Energy Procedia* **79**, 189–194 (2015).
24. Moumouni, Y., Ahmad, S. & Baker, R. J. A system dynamics model for energy planning in Niger. *Int. J. Energy Power Eng.* **3**, 308–322 (2014).
25. Khosla, R., Agarwal, A., Sircar, N. & Chatterjee, D. The what, why, and how of changing cooling energy consumption in India's urban households, *Environ. Res. Lett.* **16**, 044035 (2021).
26. Al-Hadhrami, L. M. Comprehensive review of cooling and heating degree days characteristics over Kingdom of Saudi Arabia. *Renew. Sustain. Energy Rev.* **27**, 305–314 (2013).
27. Radhi, H. Evaluating the potential impact of global warming on the UAE residential buildings - A contribution to reduce the CO2 emissions. *Build. Environ.* **44**, 2451–2462 (2009).
28. Khandker, S. R., Barnes, D. F. & Samad H. A. Are the energy poor also income poor? Evidence from India. *Energy Policy* **47**, 1–12 (2012).
29. Biarreau, L. T. et al. Heat exposure and global air conditioning. *Nat. Sustain.* **3**, 25–28 (2020).
30. Andrijevic, M. et al. *Environ. Res. Lett.* **16** 094053 <https://doi.org/10.1088/1748-9326/ac2195>, (2021).
31. Hersbach, H. et al. The ERA5 Global Reanalysis. *Q. J. R. Meteorol. Soc.* <https://doi.org/10.1002/qj.3803> (2020).
32. IEA - CMCC International Energy Agency, Weather for energy tracker. (<https://www.iaea.org/articles/weather-for-energy-tracker>) (2020).
33. NASA SEDAC Center for International Earth Science Information Network - Columbia University, Gridded Population of the World Version 4: Population Count (Revision 11 - NASA Socioeconomic Data and Applications Center, (<https://doi.org/10.7927/H4JW8BX5>), (2018).
34. Luong, N.D. A critical review on Energy Efficiency and Conservation policies and programs in Vietnam. *Renew. Sustain. Energy Rev.* **52**, (2015).
35. Corral, A. Long-Term Clustering, Scaling, and Universality in the Temporal Occurrence of Earthquakes. *Physical Review Letters* **92**, 108501 (2004).
36. Rice, J. D., Strawderman, R. L. & Johnson, B. A. Regularity of a renewal process estimated from binary data. *Biometrics* **74**, 566–574 (2018).
37. Barton, Y. et al. Clustering of Regional-Scale Extreme Precipitation Events in Southern Switzerland. *Mon. Weather Rev.* **114**, 347–369 (2016).

Acknowledgements

This research was partially supported by the EU-funded Climate Intelligence (CLINT) project. [grant agreement ID:101003876; <https://doi.org/10.3030/101003876>].

Author contributions

E.S. designed the analysis and wrote the manuscript. O.C. performed the analysis and participated to writing the manuscript. S.G. and R.Q. participated to the design of the analysis. F.M., A.B. and A.M.R. postprocessed and prepared the data together with the provision of some of the figures.

Competing interests

The authors declare no competing interests.

Additional information

Supplementary information The online version contains supplementary material available at <https://doi.org/10.1038/s43247-023-00878-3>.

Correspondence and requests for materials should be addressed to Enrico Scoccimarro.

Peer review information *Communications Earth & Environment* thanks Alessio Muscillo and the other, anonymous, reviewer(s) for their contribution to the peer review of this work. Primary Handling Editors: Alessandro Rubino, Heike Langenberg. A peer review file is available.

Reprints and permission information is available at <http://www.nature.com/reprints>

Publisher's note Springer Nature remains neutral with regard to jurisdictional claims in published maps and institutional affiliations.



Open Access This article is licensed under a Creative Commons Attribution 4.0 International License, which permits use, sharing, adaptation, distribution and reproduction in any medium or format, as long as you give appropriate credit to the original author(s) and the source, provide a link to the Creative Commons license, and indicate if changes were made. The images or other third party material in this article are included in the article's Creative Commons license, unless indicated otherwise in a credit line to the material. If material is not included in the article's Creative Commons license and your intended use is not permitted by statutory regulation or exceeds the permitted use, you will need to obtain permission directly from the copyright holder. To view a copy of this license, visit <http://creativecommons.org/licenses/by/4.0/>.

© The Author(s) 2023